Journal of Fluorine Chemistry 130 (2009) 1111–1116

Contents lists available at ScienceDirect

Journal of Fluorine Chemistry

journal homepage: www.elsevier.com/locate/fluor

Fluorination effects of MWCNT additives for EMI shielding efficiency by developed conductive network in epoxy complex

Ji Sun Im [a], In Jun Park [b], Se Jin In [c], Taejin Kim [d], Young-Seak Lee [a,*]

[a] Department of Fine Chemical Engineering and Applied Chemistry, BK21-E²M, Chungnam National University, Daejeon 305-764, Republic of Korea
[b] Biorefinery Research Center, Korea Research Institute of Chemical Technology, Daejeon 305-343, Republic of Korea
[c] Department of Fire and Disaster Protection Engineering, Woosong University, Daejeon 300-718, Republic of Korea
[d] Core Technology Research Center for Fuel Cell, Jeollabuk-do 561-844, Republic of Korea

ARTICLE INFO

Article history:
Received 19 May 2009
Received in revised form 25 June 2009
Accepted 27 June 2009
Available online 5 July 2009

Keywords:
Fluorination
CNT
Epoxy
EMI shielding

ABSTRACT

To improve the efficiency in shielding electromagnetic interference in electronic devices, multi-walled carbon nanotubes were used, due to their excellent electric and magnetic properties at high aspect ratios, and were added to an epoxy matrix. Fluorination was carried out to achieve excellent dispersion and adhesion of the additives in the epoxy matrix. The improved dispersion was confirmed by UV spectra. The permittivity and permeability were also significantly improved based on the effects of the additives and the fluorination treatment. The efficiency of shielding electromagnetic interference increased up to 28 dB. This improved efficiency of shielding electromagnetic interference may be caused by a well-organized conductive network of additives in epoxy.

1. Introduction

Recently, electronic devices and components have been rapidly developing and advancing. Thus, with increased usage of electronic devices, electromagnetic waves generated by electronic systems can potentially create serious problems such as malfunctions of medical apparatus and industry robots and can even cause harm to the human body. Therefore, electromagnetic interference (EMI) shielding materials have been investigated [1–3].

EMI can be shielded by the reflection and adsorption of electromagnetic radiation. In the past, metals have been primarily applied for EMI shielding by the reflection of electromagnetic radiation. However, metals have several disadvantages, including high density, proneness to corrosion and physical rigidity. As an alternative, composites with conducting fillers such as metal particles, carbon black, carbon fibers and carbon nanotubes (CNTs) have been extensively employed for EMI shielding [4–6].

Before selecting conducting fillers, three primary conditions have to be addressed. The first is that the material must have excellent electrical conductivity and magnetic properties. The second requirement is a high aspect ratio, which can provide a continuously conductive network via interconnection. The last one is excellent dispersion and adhesion in a matrix, which is a highly investigated topic that has not yet been met with a real solution [7]. Among the above three requirements, the first and second can be solved by the appropriate selection of additive materials; however, the last one remains a problem for the use of conducting fillers.

To address this problem, fluorination surface treatment of carbon materials has been recently investigated based on functional groups, which can change the properties of the surface [8,9]. The direct fluorination method under a gas reaction has received especially large amounts of attention due to its potential for uniform modification, efficiency, short reaction times and low cost.

In our study, we attempted dispersion by direct fluorination treatment on the surface of CNTs, which have excellent electrical conductivity and magnetic properties, low density and a high aspect ratio [10–12]. We also investigated fluorination effects on multi-walled CNT (MWCNT) additives with respect to the EMI shielding efficiency by the developed conductive network in epoxy.

2. Materials and methods

2.1. Materials

Diglycidyl ether of bisphenol A (DGEBA) (YD128, viscosity: 11,500–13,500 cps, Kukdo Chemical Co Ltd., Korea) was used as the epoxy monomer. Triarylsulfonium hexafluoro-phosphate (mixed, 50% in propylene carbonate, Aldrich Chemical Co.) was used as the photo-initiator. Multi-walled carbon nanotubes (MWCNTs, inner

* Corresponding author. Tel.: +82 42 821 7007; fax: +82 42 822 6637.
E-mail address: youngslee@cnu.ac.kr (Y.-S. Lee).

0022-1139/$ – see front matter © 2009 Elsevier B.V. All rights reserved.
doi:10.1016/j.jfluchem.2009.06.022

diameter: 2–15 nm, length: 1–10 μm, Aldrich Co.) were used as the conducting filler. Fluorine (Messer Grieheim GmbH, 99.8%) and argon (99.999%) gas were used for surface treatment.

2.2. Fluorination of MWCNTs

Fluorination of the surface of MWCNTs was carried out by a fluorination apparatus, which consists of a reactor, a vacuum pump and buffer-tank-connected gas cylinders. The conditions for fluorination were determined by trial and error to create fluorinated MWCNTs with a hydrophobicity similar to that of the epoxy. The contact angle of the epoxy was 65.5°. The fluorination conditions of the MWCNTs were then determined to obtain a similar contact angle. MWCNTs were loaded onto a nickel boat in the reactor and were degassed at 473 K for 2 h. Fluorination treatment was carried out at 303 K for 5 min at 0.5 and a total pressure of 1 bar by using mixed gas (fluorine:argon = 1:1, vol%). More details can be found in our previous work [13]. Non-treated MWCNTs and fluorinated MWCNTs treated at different pressures are referred to as follows: R-MWCNTs, F05-MWCNTs and F10-MWCNTs, respectively.

2.3. Blend preparation

A certain amount of MWCNTs (0.02 g) was dispersed in ethanol (50 ml). In order to release the bundles, the MWCNT and ethanol mixture was sonicated for 3 h. Next, the epoxy monomer (20 g) was added into the mixture and stirred at 2000 rpm for 4 h. After stirring, in order to remove the ethanol, the mixture was kept at 80 °C in an oven for 6 h.

2.4. Procedure of irradiation curing

The photo-initiator (1 g) was added into the prepared blend and then stirred at 2000 rpm and 70 °C for 5 h. The blend was poured into a 150 mm × 150 mm × 2 mm aluminum mold that was treated with a release agent. The mold was then placed under an E-beam accelerator (ELV-4, EB Tech Co., Korea) (energy: 2.5 MeV, current: 7.5 mA). E-beams were irradiated at a dose rate of 300 kGy/h in atmosphere for 10 min.

2.5. Characterization of samples

UV spectrometry (Optizen 2120 UV, Mecasys, Korea) was used to investigate the dispersion of CNTs in ethanol. The measurement was carried out following the general method presented by other groups [14]. Measurements were acquired at 635 nm after sonication for 1 h.

In order to investigate fluorination effects on the MWCNTs, the change of surface morphology was investigated by field-emission transmission electron microscope apparatus (FE-TEM, JEM-2100F HR) at 200 kV.

The oriented and defected carbon structures were examined using Raman analysis to determine the effects of heat treatment temperature and fluorination. Raman spectral analysis was conducted with an excitation power of 10 mW at 514 nm (RM 1000-InVia, Renishaw).

The XPS spectra of the MWCNTs used in this study were obtained with a MultiLab 2000 spectrometer (Thermo Electron Co., England) to evaluate the changes of chemical species on the surface of the MWCNTs before and after fluorination. Al Kα (1485.6 eV) X-rays were used with a 14.9-keV anode voltage, a 4.6-A filament current and a 20-mA emission current. All samples were treated at 10^{-9} mbar to remove impurities. The survey spectra were obtained with a 50-eV pass energy and a 0.5-eV step size. Core level spectra were obtained at a 20-eV pass energy with a 0.05-eV step size.

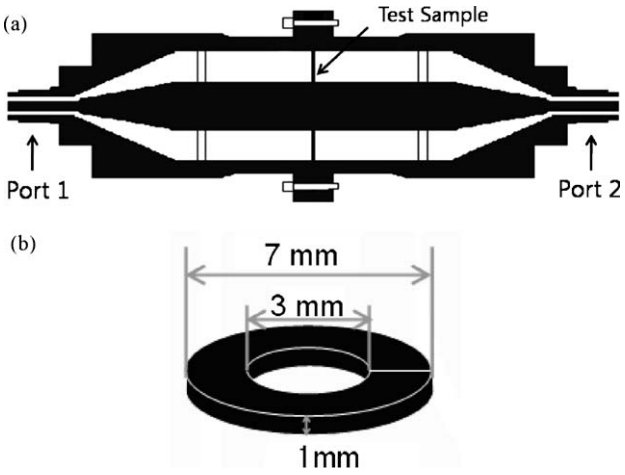

Fig. 1. Structure of the EMI SE holder (a) and the shape and dimensions of the EMI SE test specimen (b).

Permittivity, magnetic permeability and EMI shielding efficiency (SE) were obtained according to the ASTM D-4935-99 method using a network analyzer (Agilent, E5071A) equipped with an amplifier and a scattering parameter (*S*-parameter) test set over a frequency range of 800 MHz–4 GHz [15]. Annular disks were prepared with a punching machine and were installed into the test tool as shown in Fig. 1. The EMI SE was calculated using *S* parameters via equations found in the literature [16].

3. Results and discussion

3.1. Effects of fluorination on the dispersion of MWCNTs in ethanol

The dispersion stability of MWCNTs is an important factor in uniformly manufacturing MWCNTs dispersed in epoxy. The electrochemical properties of the resultant sample will be strongly influenced by the dispersion stability of the MWCNTs. The improved dispersion of the MWCNTs in ethanol can be observed from the UV spectra shown in Fig. 2. At all times, the transmitted intensity is lower with fluorination treatment, as seen by comparing the R-MWCNTs and F05-MWCNTs, indicating that the dispersion was improved by fluorinating the MWCNTs to match the hydrophobicity of ethanol Under higher fluorination pressure, more improved dispersion was observed in the

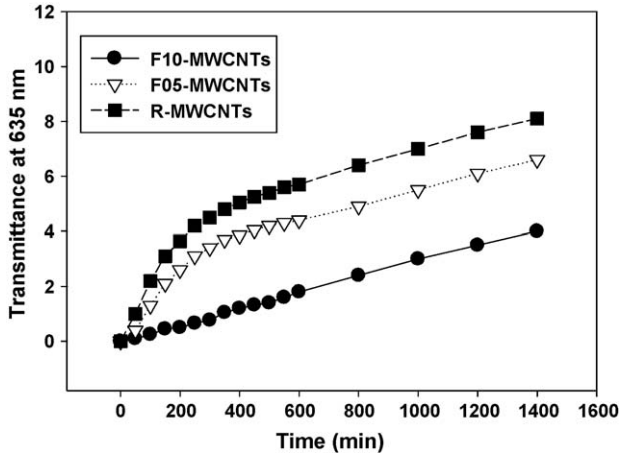

Fig. 2. Dispersion of fluorinated MWCNTs measured by IR.

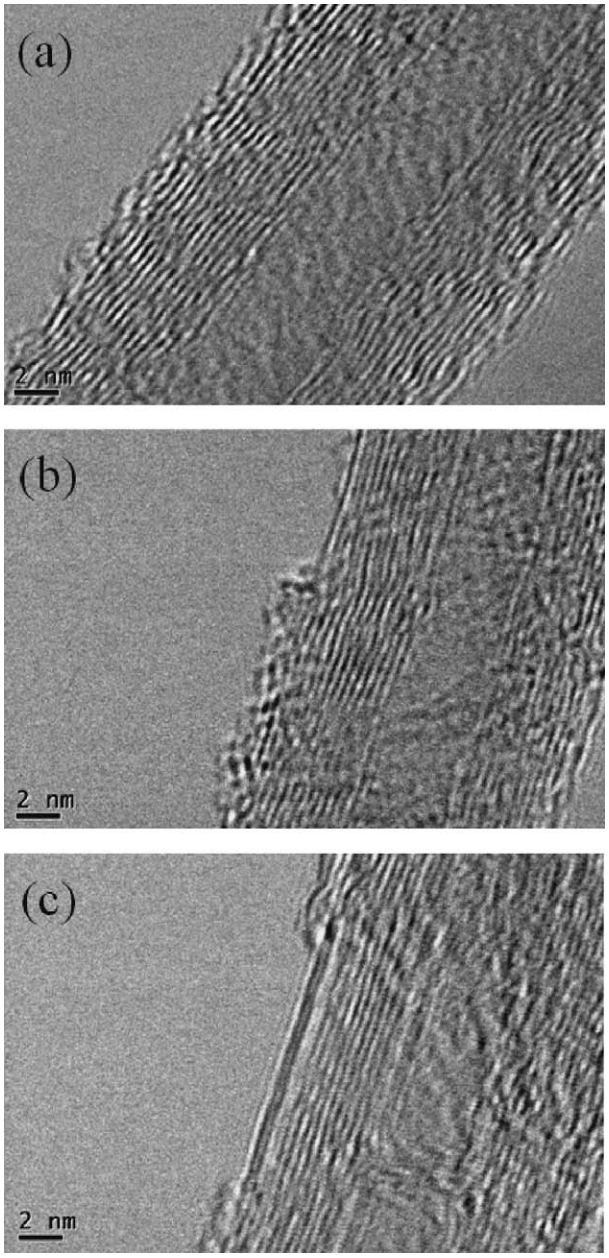

Fig. 3. Changes of surface morphology by fluorination: (a) R-MWCNTs, (b) F05-MWNCTs and (C) F10-MWCNTs.

F10-MWCNTs. This result can be explained by the fact that hydrophobic groups functionalized by fluorination treatment lead to an excellent interface match between ethanol and fluorinated MWCNTs.

3.2. Surface morphology of fluorinated MWCNTs

The change of surface morphology was investigated by TEM images in Fig. 3. Even though the significant change was not found roughly, some of amorphous carbon structures on the outside of wall were removed through fluorination treatment. In detail, the R-MWCNTs showed the amorphous carbon layer on the outside of wall in Fig. 3(a). In case of the F05-MWCNTs, it can be observed that some of amorphous carbon layer was reduced. Finally, the cleaning effects can be observed in case of the F10-MWCNTs. It can be said that etching effects were carried out on the surface of MWCNTs by fluorination treatment.

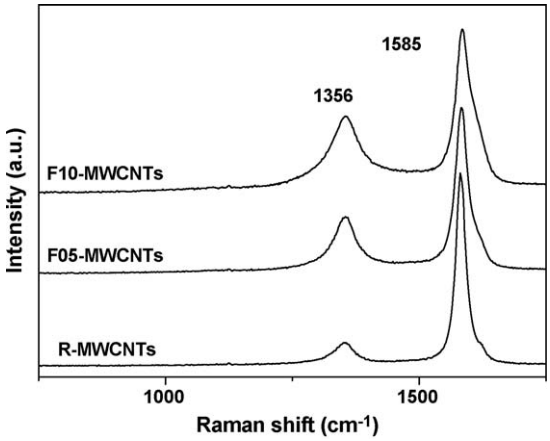

Fig. 4. Raman spectra of fluorinated MWCNTs.

3.3. Defect and graphite structures

Raman spectra of the MWNCTs are presented in Fig. 4 to illustrate the defect and graphite structures. In three samples, peaks related to defect and graphite structures (called *D* and *G* peaks) were observed at 1356 and 1585 cm^{-1}, respectively. The *D* peak increased with fluorination, with a decrease in the *G* peak, indicating that fluorination treatment destroys the graphite structure of MWCNTs. The Ig/Id (intensity of graphite/intensity of defects) ratios of the R-MWCNTs, F05-MWCNTs and F10-MWCNTs were 8.61, 3.27 and 2.25, respectively. Thus, the initial change in fluorination pressure affects the structure of MWCNTs.

3.4. Chemical bonds by fluorination

Elemental analysis measured by XPS survey is presented in Fig. 5. The strongest peak corresponded to C1s from the MWCNTs in all samples, and with the fluorination treatment, F1s and F KL1 were observed, indicating the existence of fluorine on the surface of the MWNCTs. The atomic composition of the R-MWCNTs was 96.9% carbon and 3.1% oxygen. This oxygen may come from the environmental atmosphere. In the case of the fluorinated MWCNTs, the carbon, oxygen and fluorine contents of the F05-MWCNTs and F10-MWCNTs were 93.0%, 2.7% and 4.3% and 91.5%, 3.1% and 5.4%, respectively.

Fig. 6 shows the C1s deconvolution performed to investigate the chemical bonds on the surface of the MWCNTs. C1s peaks were deconvoluted to several pseudo-Vogit functions (sums of the Gaussian–Lorentzian function) with a peak analysis program obtained from Unipress Co., USA. The pseudo-Vogit function is given by [17]:

$$F(E) = H\left[(1-S)\exp\left(-\ln(2)\left(\frac{E-E_0}{\mathrm{FWHM}}\right)^2\right) + \frac{S}{1+\left(\frac{E-E_0}{\mathrm{FWHM}}\right)^2}\right]$$

where $F(E)$ is the intensity at energy E, H is the peak height, E_0 is the peak center, FWHM is the full width at half maximum, and S is the shape function related to the symmetry and Gaussian–Lorentzian mixing ratio. The components of C are presented with the binding energy in Table 1. In the case of the R-MWCNTs, C(1), C(2) and C(3) were observed at 284.5, 285.1 and 286.2 eV, related to sp^2, sp^3 carbon and sp^3 carboxyl groups, respectively. Via fluorination treatment, C(4), C(5) and C(6) were generated at 287.5, 288.5 and 290.7 eV, related to semi-ionic C–F, nearly covalent C–F and covalent C–F (CF_2, CF_3), respectively. With fluorination, semi-ionic

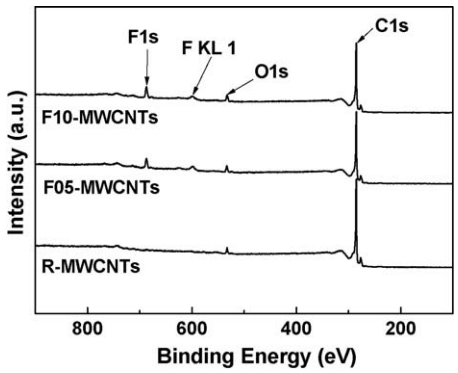

Fig. 5. Elemental analysis by XPS survey peaks.

and covalent bonds between carbon and fluorine developed, as shown in Table 1.

3.5. Permittivity and magnetic permeability analysis

The permittivity of the samples is presented in Fig. 7. In all of the samples, the real permittivity of the sample was higher than the imaginary permittivity. After considering which of the real and imaginary permittivities is related to storage and loss effects [18,19], it was determined that the storage effect is larger than the loss effect. This behavior would result in absorbing, rather than reflecting, the EMI. The epoxy showed an average real permittivity of about 0.9, and the composite of the R-MWCNTs, and epoxy exhibited a value around 1.9, an increase of more than a factor of 2. The average real permittivity increased up to 2.7 in the composite of the F10-MWCNTs and epoxy because the dispersion of MWCNTs may be improved in the epoxy matrix by the fluorination of MWCNTs. In addition, it can be expected that the adhesion can be improved by hydrophobic groups functionalized by fluorination treatment based on the similar hydrophobicity between the epoxy and fluorinated MWCNTs. The fluorination effects for improved adhesion properties have been presented also by other groups with consideration of surface energy changes [20,21].

The permeability of the samples is shown in Fig. 8. Corresponding with the results of permittivity, the real permeability was higher than the imaginary permeability, and it increased with the addition of MWNCTs and the effect of fluorination treatment. This is caused by the excellent magnetic properties of MWCNTs [22]. The average real magnetic permeability improved up to 1.3 and 2.3 by the addition of the R-MWCNTs and F-10 MWCNTs, respectively.

3.6. EMI SE analysis

The EMI SE measured from 800 to 4000 MHz is shown in Fig. 9. In the case of the epoxy, the average EMI SE was about

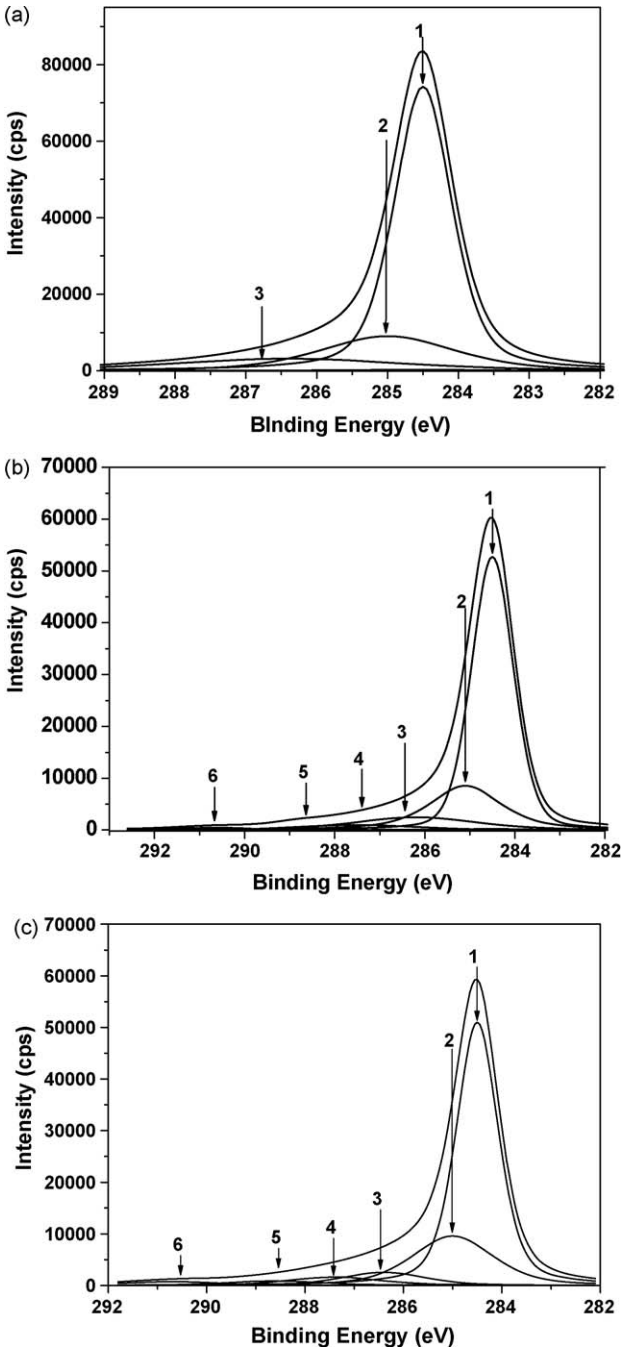

Fig. 6. C1s deconvolution: (a) R-MWCNTs, (b) F05-MWNCTs and (C) F10-MWCNTs.

Table 1
C 1s spectra and assignment.

Component	Binding energy (eV)	Assignment	Concentration (%)		
			R-MWCNTs	F05-MWCNTs	F10-MWCNTs
C(1)	284.5	sp^2 carbon	68.8	63.9	62.3
C(2)	285.1	sp^3 carbon	19.4	20.7	22.5
C(3)	286.2	O–C(carboxyl)	11.8	9.7	6.1
C(4)	287.5	Semi-ionic C–F	–	3.7	4.4
C(5)	288.85	Nearly covalent C–F	–	0.8	2.5
C(6)	290.7	Covalent C–F(CF_2, CF_3)	–	1.1	2.1

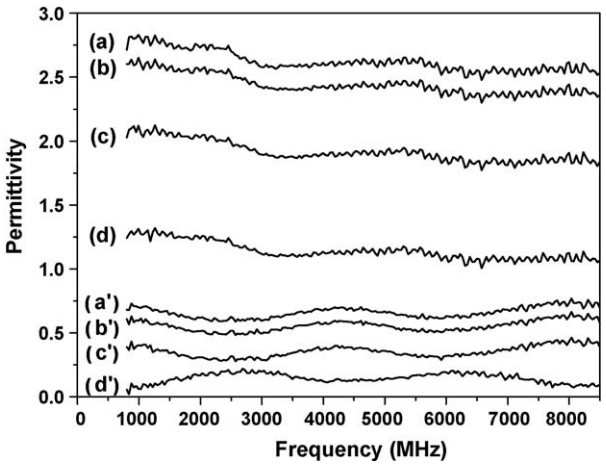

Fig. 7. Permittivity of samples; (a) and (a′): real and imaginary permittivity of F10-MWCNTs/epoxy, (b) and (b′): real and imaginary permittivity of F05-MWNCTs/epoxy, (c) and (c′): real and imaginary permittivity of R-MWCNTs/epoxy, (d) and (d′): real and imaginary permittivity of epoxy.

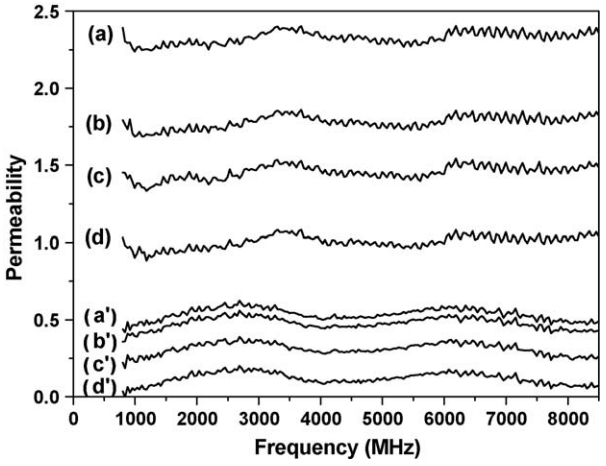

Fig. 8. Permeability of samples; (a) and (a′): real and imaginary permeability of F10-MWCNTs/epoxy, (b) and (b′): real and imaginary permeability of F05-MWNCTs/epoxy, (c) and (c′): real and imaginary permeability of R-MWCNTs/epoxy, (d) and (d′): real and imaginary permeability of epoxy.

10 dB, and the EMI SE decreased significantly, by about 80%, over 3000 MHz. The EMI SE was improved by the addition of MWCNTs in the composite of R-MWNCTs/epoxy, showing an average of around 17 dB. In the case of the addition of the

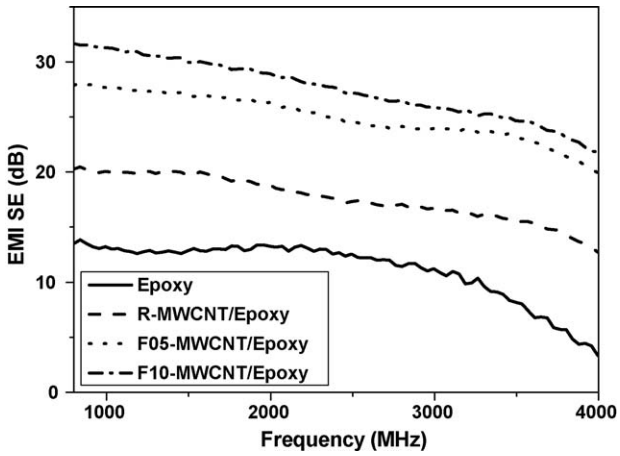

Fig. 9. EMI SE of epoxy/MWCNT composites.

F05-MWCNTs and F10-MWCNTs, the average EMI SE was 25 and 28 dB, respectively. Another striking result is that the decreasing phenomenon of the EMI SE over 3000 MHz was efficiently reduced by the addition of MWNCTs. Overall, the EMI SE was improved due to effects of the MWCNTs and fluorination treatment.

3.7. Suggested mechanism of dispersion effects by fluorination for EMI SE

The suggested EMI shielding mechanism is presented in Figs. 10 and 11. Figs. 10(a) and 11(a) show the orientation of electrons caused by the permittivity of the MWCNTs and the fluorinated MWCNTs under an outside electromagnetic force, expressed by seven arrow lines. By orienting the electrons in each MWCNT, the inner electric resistance would be generated against the outside applied electric field with an opposite direction, as shown in Figs. 10(b) and 11(b). In this case, fluorinated MWCNTs can cause a more efficient internal electric resistance, resulting from the effectively connected MWCNTs. This result is based on the excellent dispersion of MWCNTs caused by the fluorination surface treatment. Eventually, the EMI might be shielded more efficiently, as shown in Figs. 10(c) and 11(c). It can be concluded that fluorination surface treatment of MWCNTs causes the improved dispersion of MWCNTs and that well-dispersed MWCNTs lead to highly oriented electrons by the nature of the permittivity of MWCNTs. This phenomenon contributed to a more efficient internal electric resistance against an externally applied electric field and to a highly improved EMI SE.

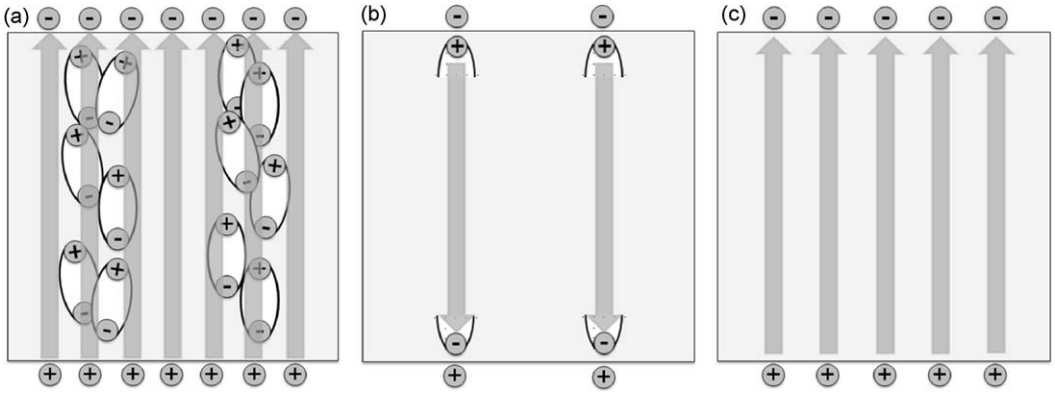

Fig. 10. Suggested EMI shielding mechanism of the composite of MWCNTs/epoxy.

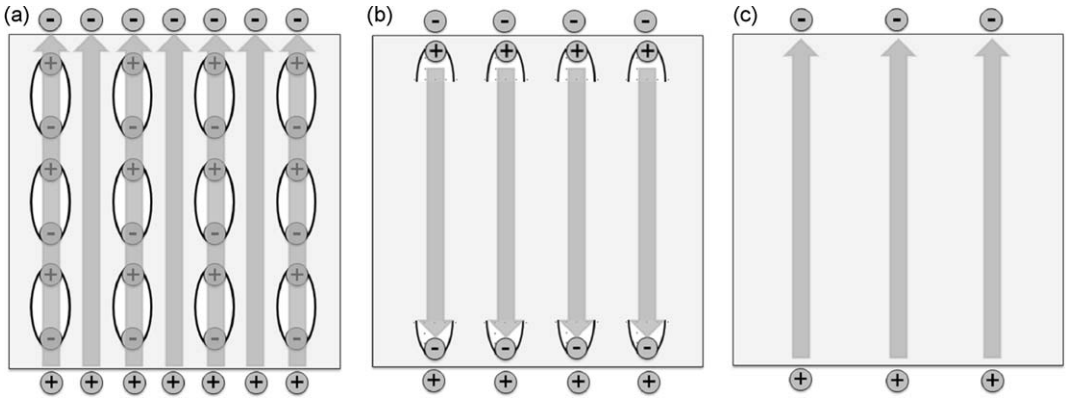

Fig. 11. Suggested EMI shielding mechanism of the composite of fluorinated MWCNTs/epoxy.

4. Conclusions

The efficiency of shielding electromagnetic interference in epoxy was improved by the effects of MWCNT additives and their surface treatment by fluorination. This result may be due to the excellent electrical and magnetic properties of MWCNTs and the good dispersion and adhesion of MWCNTs in an epoxy matrix achieved by fluorination. The dispersion of MWCNTs was improved by a factor of 2.5, as measured by UV spectra. The permittivity and permeability were also improved, contributing to a high EMI SE. Eventually, the EMI SE of the composite of the F-10 MWCNTs and epoxy reached up to 28 dB, improving by a factor of about 2.8, as compared with epoxy. This result can be explained by the fluorination effects of improved dispersion and adhesion between fluorinated MWCNTs and epoxy by introducing hydrophobic functional groups via fluorination treatment.

Acknowledgement

This research was supported by a grant from the Fundamental R&D Program for Core Technology of Materials funded by the Ministry of Knowledge Economy, Republic of Korea.

References

[1] W.S. Jou, H.Z. Cheng, C.F. Hsu, J. Alloys Compd. 434–435 (2007) 641–645.
[2] Q. Hu, M.S. Kim, Carbon Lett. 9 (2008) 298–302.
[3] L. Martzui, L. Vovchenko, Y. Prylutskyy, I. Korotash, V. Marzui, P. Eklund, U. Ritter, P. Scharff, Mater. Sci. Eng. C 27 (2007) 1007–1009.
[4] K.Y. Park, S.E. Lee, C.G. Kim, J.H. Han, Compos. Struct. 81 (2007) 401–406.
[5] J.S. Im, J.G. Kim, Y.S. Lee, Carbon 47 (2009) 2640–2647.
[6] Y. Huang, N. Li, Y. Ma, F. Du, F. Li, X. He, X. Lin, H. Gao, Y. Chen, Carbon 45 (2007) 1614–1621.
[7] M.S. Han, Y.K. Lee, H.S. Lee, C.H. Yun, W.N. Kim, Chem. Eng. Sci., in press.
[8] Y.S. Lee, T.H. Cho, B.K. Lee, J.S. Rho, K.H. An, Y.H. Lee, J. Fluor. Chem. 120 (2003) 99–104.
[9] J.S. Im, S.J. Park, Y.S. Lee, Int. J. Hydrogen Energy 34 (2009).
[10] S.J. Park, S.Y. Lee, Carbon Lett. 10 (2009) 19–22.
[11] C.S. Zhang, Q.Q. Ni, S.Y. Fu, K. Kurashiki, Compos. Sci. Technol. 67 (2007) 2973–2980.
[12] S.J. Kim, J.S. Im, P.H. Kang, T. Kim, Y.S. Lee, Carbon Lett. 9 (2008) 294–297.
[13] J.M. Lee, S.J. Kim, J.W. Kim, P.H. Kang, Y.C. Nho, Y.S. Lee, J. Ind. Eng. Chem. 15 (2009) 66–71.
[14] O.K. Park, T. Jeevananda, N.H. Kim, S.I. Kim, J.H. Lee, Scripta Mater. 60 (2009) 551–554.
[15] Y.K. Hong, C.Y. Lee, C.K. Jeong, D.E. Lee, K. Kim, J. Joo, Rev. Sci. Instrum. 74 (2003) 1098–1102.
[16] A.M. Nicolson, G.F. Ross, IEEE Trans. Instrum. Meas. 19 (1970) 377–382.
[17] Z. Wu, J. Li, D. Timmer, K. Lozano, S. Bose, Int. J. Adhes. Adhes. 29 (2009) 488–494.
[18] W.B. Weir, Proc. IEEE 62 (1974) 33–36.
[19] J.B. Jarvis, M.D. Janezic, J.H. Grosvensor, R.G. Geyer, Transmission/Reflection and Short-Circuit Line Methods for Measuring Permittivity and Permeability, Natl. Inst. Stand. Technol., Washington, 1993, pp. 52–65.
[20] F.J. du Toit, R.D. Sanderson, J. Fluorine Chem. 98 (1999) 115–119.
[21] K.K.C. Ho, S. Lamoriniere, G. Kalinka, E. Schulz, A. Bismarck, J. Colloid Interface Sci. 313 (2007) 476–484.
[22] M.S. Dresselhaus, G. Dresselhaus, P.C. Eklund, Science of Fullerences and Carbon Nanotubes, Academic Press, San Diego, 1996.